

---

## Original Paper

---

# Effect of Surface Defects on FRP-Concrete Interface Bond Strength

Nur Yazdani<sup>1</sup>, Mina W. Riad<sup>2</sup>, Romy Salloum<sup>3</sup>, Rebecca B. Carr<sup>4</sup>

<sup>1</sup>Professor, Department of Civil Engineering, University of Texas at Arlington, Box 19308, Arlington, TX 76019, U.S.A;

<sup>2</sup>Senior Structural Designer, HSA and Associates, 1906 W Garvey Ave S., #200, West Covina, CA 91790, USA;

<sup>3,4</sup>Undergraduate Research Assistant, Department of Civil Engineering, University of Texas at Arlington, Box 19308, Arlington, TX 76019, U.S.A;

### Abstract

Carbon Fiber Reinforced Polymer (CFRP) laminates have been successfully used as externally bonded reinforcements for retrofitting, strengthening and confinement of concrete structures. The adequacy of the CFRP-concrete bonding largely depends on the bond quality and integrity. The bond quality may be compromised during the CFRP installation process due to various factors. In this study, the effect of four such construction-related factors were assessed through various laboratory destructive testing methods, and quantification of any detrimental effects was achieved. The factors were: surface voids, surface wetness, upward vs. downward CFRP application, and surface cleanliness. A common unidirectional CFRP was applied to small scale flexural concrete samples with induced surface defects. Schmidt Hammer, pull-off testing and flexural testing were employed to determine possible detrimental effect of the induced parameters on the bond quality and flexural failure load. The Schmidt Hammer approach was found to be inconsistent for application on the CFRP surface. Pull-off and flexural testing showed that surface wetness, cleanliness and upward CFRP application cause minor reduction in the bond tensile and bending strengths, in the range of 3 – 9%. This is possibly due to premature CFRP debonding failure at the epoxy interface. Small surface air voids below the CFRP (less than around 2% of the CFRP area) cause minor bond strength reduction and may be neglected.

**Keywords:** CFRP laminate, CFRP-concrete bond, Concrete surface defects, CFRP debonding, Flexural capacity

---

## 1. Introduction

Carbon Fiber Reinforced Polymer (CFRP) external laminate is widely used to strengthen and confine concrete structures for strength and durability. The adequacy of the externally bonded FRP strengthening mechanism depends on the quality of the concrete-CFRP bond. Ideally, FRP laminate that is perfectly bonded to the concrete surface without any debonding, delamination or air bubbles is desirable. However, during the installation process, various factors may cause such defects and result in bond loss. The quality of the interfacial bond ensures satisfactory performance of the FRP strengthened structure.

Non-destructive Evaluation (NDE) methods may be used to qualitatively or quantitatively evaluate the interfacial bond between FRP and the concrete substrate for both existing and new structures. NDE methods such as thermography, ultrasonic C-scan, acousto-ultrasonic, impact-echo, microwave, ground penetrating radar (GPR), eddy current and laser shearography were used previously to scan and image three pre-cracked reinforced concrete beams with externally applied FRP laminates [1, 2, 3]. Thermography is particularly effective in identifying actual or potential weak or missing bond areas due to construction defects or imperfections. It has been used to monitor CFRP strengthened reinforced concrete bridge columns, bridge decks, and reinforced concrete beams [4, 5, 6, 7, 8]. However, it may be difficult to predict the in-service interfacial bond strength from such NDE scanning.

Incomplete bonding or lamination at the FRP-concrete interface can be due to installation related factors or environmental factors. Such factors may decrease any CFRP strengthening and confining contribution to the concrete structure that is considered in design (such as flexural, shear and axial capacities). Designers typically assume a perfect bond between the CFRP and the concrete substrate in capacity calculations. Quantification of such related factors will allow any needed reductions in the capacity contributions of the FRP to the concrete substrate, assuring safety and integrity of the structure. No study has been conducted to date on the quantitative determination of any such detrimental factors on the FRP-concrete bond capacity.

In the study reported herein, four common and likely construction related factors were considered in an experimental determination of the effect of these factors on FRP-concrete bond strength, as follows:

1. Concrete surface voids: Voids can be present on or near the concrete surface due to air bubbles in wet concrete and formwork imperfections. If the voids are left unpatched prior to the FRP application, some interfacial bonding and strength may be lost.
2. Concrete surface wetness: Wet concrete surface due to rain or water leakage may result in weak bonding or bubbles, and evaporation of this water may cause localized FRP debonding. If the wet concrete surface is not allowed to completely dry out before the FRP application due to time constraints or oversight, it could be detrimental for bond quality. Surface moisture and wetness, and effect of presence water, were found to have an adverse effect on the bond durability between CFRP and concrete (Tuakta and Büyüköztürk, 2011; Wan et al., 2006).
3. Upward vs. downward CFRP application: During flexural and shear strengthening of overhead concrete members (such as bridge girders), the FRP is normally applied upward (against gravity). However, most of the previous studies [9,10] were conducted on laboratory specimens where the FRP was applied downward on the concrete surface. The overhead application may result in inadequate bonding and strength loss due to the gravity effect.
4. Concrete surface cleanliness: This is one of the possible critical parameter that may affect the bond quality. The concrete surface may be properly roughened according to manufacturer's specifications before the epoxy-FRP application. However, if thorough cleaning to remove all loose material may be compromised, the bond quality could be adversely affected.

## 2. Material Properties and Methods

### 2.1. Sample preparation

The study utilized an experimental approach with small unreinforced concrete beams, application of CFRP on the concrete surface, and destructive flexural testing until failure to determine the ultimate loads. Plywood forms were used to cast 11 plain concrete beams of dimension 200 x 200 x 920 mm. A 100 x 200 mm cardboard piece was inserted in each fresh concrete sample to form a notch at the mid-span. Ready-mix concrete from a local concrete plant was used to ensure uniformity among samples. The samples were

moist cured for 28 days to achieve a target 28-day compressive strength of 20.7 MPa and a slump of 114 mm. The mix design is presented in Table 1.

Figures 1 and 2 show the dimensions and the finished beam samples, respectively.

**Table 1.** Concrete Mix Design

Material	kg/m <sup>3</sup>
Cement	394
Water	186
Coarse aggregate (crushed stone with maximum aggregate size 19 mm)	987
Fine aggregate (sand)	669

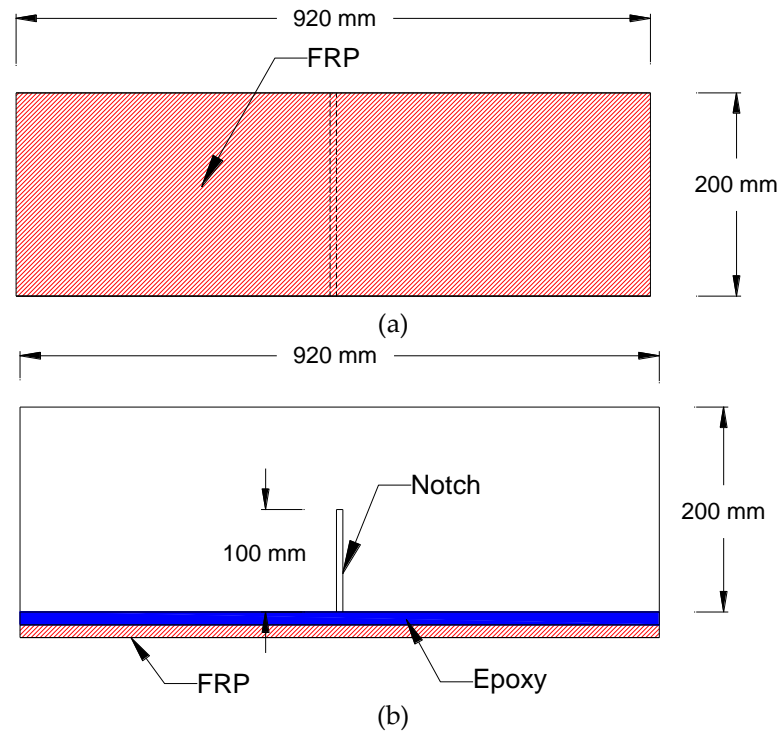


**Figure 1.** Sample Dimensions. (a) Plan; (b) Elevation



**Figure 2.** Concrete Beam Specimens

The width of each beam was chosen as 200 mm in order to accommodate the GPR antenna size, while the depth and length were selected following ACI 440 [18] guidelines to make sure that the load testing failure occurred in the FRP concrete interface. As the capacity of the bond is directly proportional to the concrete strength, the design was based on a concrete compressive strength ( $f'_c$ ) of 24.1 MPa. The failure load for the control beams was calculated as 62.2 KN, which was below the capacity of the available bending test machine. This helped in achieving a balance between a typical concrete strength and a beam size and load carrying capacity, that were handled well in testing. Equation 1 from ACI 440 [13] was used to calculate the strain level at which debonding may occur. The beam was sized to reach strain values that exceeded the ACI 440 strain limit.

$$\varepsilon_{fd} = 0.41 \sqrt{\frac{f'_c}{nE_f t_f}} \quad (1)$$

Where:

$\varepsilon_{fd}$  = debonding strain of FRP reinforcement, mm/mm

$f'_c$  = specified compressive strength of concrete, MPa

$n$  = number of plies of FRP reinforcement

$E_f$  = tensile modulus of elasticity of FRP, MPa

$t_f$  = nominal thickness of one ply of FRP reinforcement, mm

A common unidirectional CFRP laminate was applied at an ambient temperature of 16°C, in the absence of direct sunlight, to prevent any undesirable problems with the epoxy. The one-layer CFRP application completely covered one horizontal face of each sample, simulating flexural strengthening in a beam type member. The manufacturer specified values for the CFRP laminate are presented in Table 2. Figure 3 shows the application process of CFRP laminate.

**Table 2.** CFRP Cured Laminate Properties

Cured laminate properties	Design Values
Tensile Strength	724 MPa
Modulus of Elasticity	56,500 MPa
Elongation at Break	1.0%
Thickness	0.51 mm

**Figure 3.** Application of CFRP laminate

Type 1 epoxy was the major gluing agent, applied to both sides of the CFRP, and also on the concrete surface. A Hi-Mod gel, 2-component, 100% solid, solvent-free, moisture-tolerant, high-modulus, high strength, and structural epoxy paste adhesive was used, conforming to ASTM C-881 [11] and AASHTO M-235 [12] specifications. The manufacturer specified epoxy properties are presented in Table 3.

**Table 3.** Type 1 Epoxy properties

Properties	Design Values
Tensile Strength	72.5 MPa
Tensile Modulus	3174 MPa
Elongation at Break	4.8%
Flexural Strength	123.5 MPa

The selected epoxy type 2, which was compatible with the selected CFRP and type 1 epoxy, and from the same manufacturer, was used together with type 1 epoxy in case of the overhead application in samples 9 and 10. This was necessary because type 1 epoxy by itself was not sufficiently strong to overcome the gravity effect and firmly hold the CFRP sheet in place. Type 2 epoxy was a high strength, high modulus and moisture tolerant impregnating resin. The manufacturer specified epoxy properties are presented in Table 34.

**Table 4.** Type 2 Epoxy Properties

Properties	Design Values
Density	1.5 kg/L
Shrinkage	Negligible
Tensile Strength	14.8 MPa
Flexural Strength	36 MPa
Compressive Strength	70-90 MPa

Shear Strength	21 MPa
Elastic Modulus	6867-7358 MPa
Adhesion to grit blasted steel	14 MPa

The study involved a parametric combination and two sample replications for each parameter, as shown in Table 5. As stated in ACI 440 [13], the concrete surface was roughened by sandblasting to a CSP3 profile [**Error! Reference source not found.**] to facilitate good quality CFRP bonding, as shown in Figure 4.

**Table 5.** Test Matrix

Sample No.	Surface Cleanliness	Surface Wetness	Application Direction	Epoxy	Voids
1 (control)	Clean	Dry	Underhead	Type1	None
2(control)	Clean	Dry	Underhead	Type1	None
3	Clean	Dry	Underhead	Type1	Four voids (10x10 mm)
4	Clean	Dry	Underhead	Type1	Four voids (20x20 mm)
5	Clean	Dry	Underhead	Type1	Two voids (20x20 mm)
6	Clean	Dry	Underhead	Type1	Two voids (40x40 mm)
7	Clean	Wet	Underhead	Type1	None
8	Clean	Wet	Underhead	Type1	None
9	Clean	Dry	Overhead	Type1 + Type 2	None
10	Clean	Dry	Overhead	Type1 + Type 2	None



**Figure 4.** Sand Blasting of Beams

## 2.2. Parameters

### 2.2.1. Parameter 1: Surface Voids

To investigate the effect of air voids under the CFRP, a few small to large surface voids were placed on the fresh concrete for samples 3 - 6 using foam cubes (Figure 6). The void dimensions were selected to result in possible decrease in bond areas. The allowable void size under CFRP, according to ACI 440.2R [**Error! Reference source not found.**], is less than 1300 mm<sup>2</sup> each. The void sizes were 10 x 10 x 10, 20 x 20 x 20, and 30 x 30 x 30 mm, respectively. No voids were planted on the surfaces of the remaining samples.

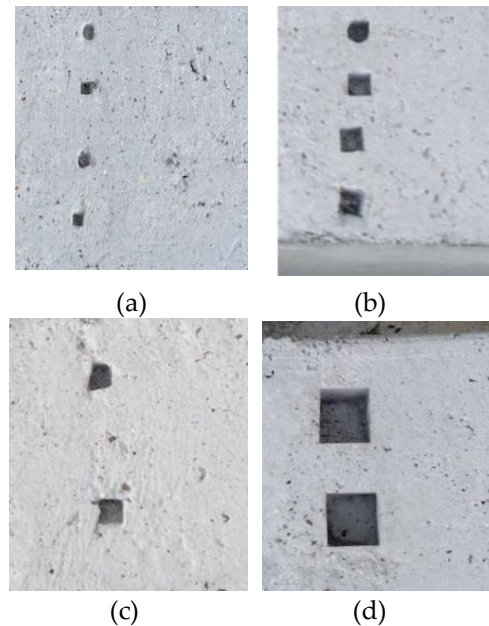


**Figure 5.** Surface Voids. (c) Sample 3 (10 mm voids); (d) Sample 4 (20 mm voids); (c) Sample 5 (20 mm voids); (d) Sample 6 (30 mm voids)

### 2.2.2. Parameter 2: Surface Wetness

The surfaces of samples 7 and 8 were saturated with sprinkled water just prior to the application of epoxy and CFRP. For other samples, no water was applied, and the surface was kept dry before the CFRP application.

### 2.2.3. Parameter 3: Upward vs. downward CFRP application

Samples 9 and 10 were supported on both ends, allowing access below the samples, as shown in Figure 5. The CFRP was then applied from below as an upward application, typical for application on the bottom flange of girders and underneath of slabs. For the other samples, the CFRP was applied from the top, as shown in Figure 3. A combination of types 1 and 2 epoxy were used herein, as discussed earlier.



**Figure 6.** Setup for Upward application of CFRP

#### 2.2.4. Parameter 4: Concrete Surface Cleanliness

After sandblasting, the concrete surfaces were cleaned well of any loose materials or dust through air blasting, for samples 1-10. For sample 11, the surface was not cleaned, and some additional dust was deliberately placed on the dry surface before the CFRP application to determine the effect of an unclean surface [14]. This represents cases where the CFRP is not applied immediately after the sandblasting operation, or improper cleaning after sandblasting.

#### 2.3. Schmidt Rebound Hammer (ASTM C805 2013)

This is a widely used testing equipment for estimation of concrete, asphalt and rock strengths. Although it is considered non-destructive, in reality it is partially destructive when used on CFRP retrofitted beams, as it ruptures the CFRP fibers. The test was done according to ASTM C805 standards as mentioned in the ACI 440.2R-17 guidelines. The test using the hammer can be seen in Figure 7 below.



Figure 7. Schmidt Hammer Test

#### 2.4. Pull off Adhesion Testing (ASTM C900-15, 2015)

The ASTM Pull-Off Testing was performed to spot check the tensile pull-off strength of the CFRP laminate with 50 mm wide dollies glued to the laminate. The maximum pull-off pressure and pull rate was recorded at two locations, 75 mm from the sample edge on each side.

#### 2.5. Flexural Testing

A three-point flexural testing protocol was adopted herein to determine the failure load of all beam samples in order to investigate any effect of the surface defects on the flexural capacity (Figure 9). All supports were made of thick steel plates to prevent deflection at the supports. A 2670 kN compression testing machine was used under a constant rate of loading. The built-in notch ensured that the failure was at the mid-span. Data was collected from a linear varying displacement transducer (LVDT) at mid-span for deflection, and two strain gages, as shown.

All tests were conducted one year after the samples were prepared.

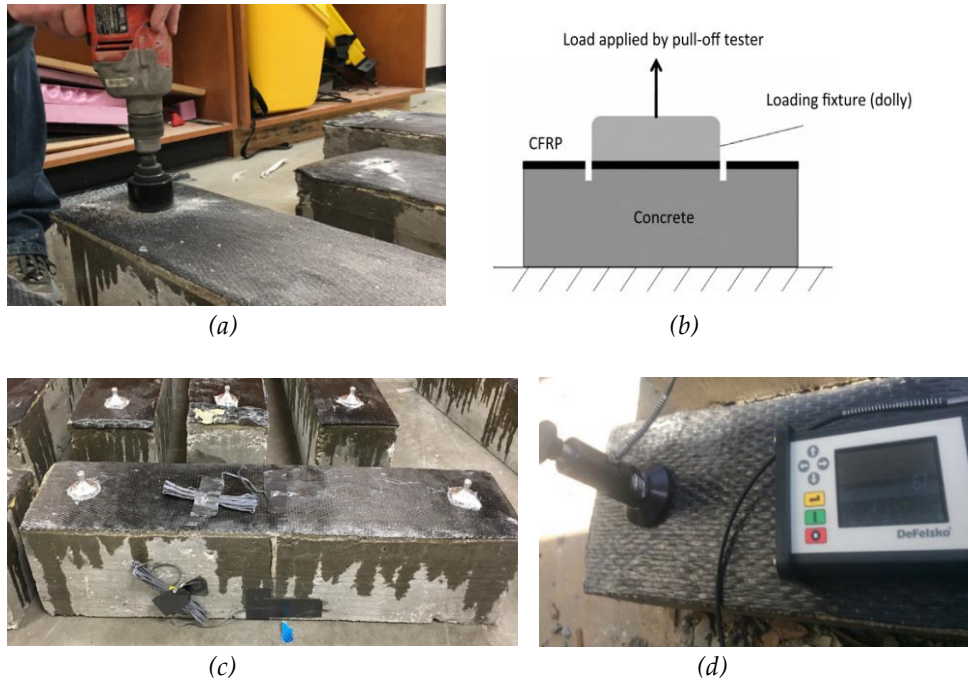


Figure 8. Pull-Off Testing. (a) Attached Dollies; (b) Mechanism; (c) Scoring; (d) Testing in Progress

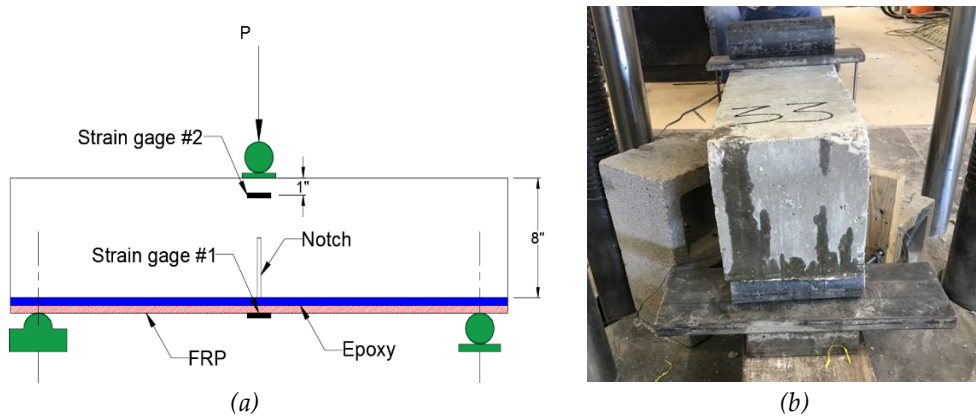


Figure 9. Three-point Bending Test Setup. (a) Schematic; (b) Actual Testing

### 3. Results and Discussion

#### 3.1. Schmidt Hammer

For the Schmidt Hammer approach, the ratio between the rebound velocity and the impact velocity is designated as the “Q” value, and the averages obtained herein are shown in Figure 10.

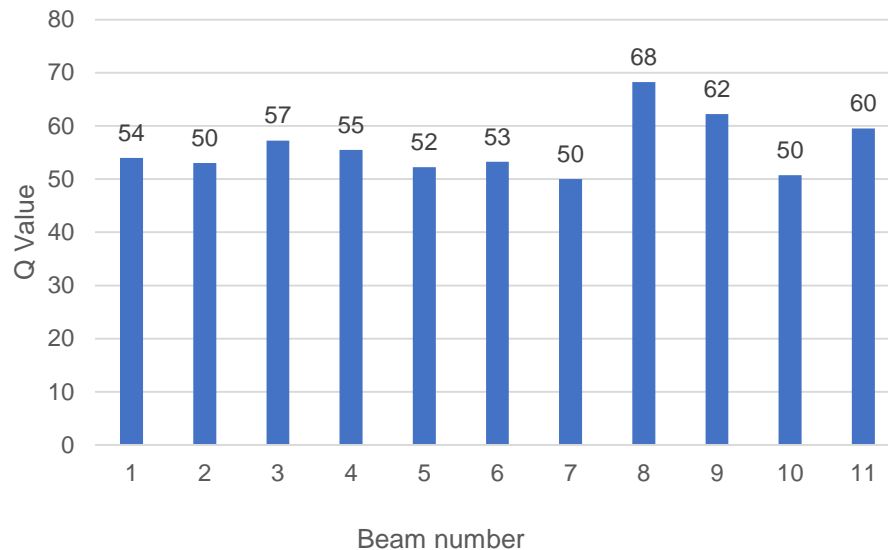


Figure 10. Schmidt Hammer Rebound Q Values

The results were found to be somewhat inconsistent. For example, Q values for control samples 1 and 2 were less than that in most other samples. These samples had no induced surface defects, and should have the highest hardness values of all samples. Samples 7 and 8 had the same parameter of surface wetness, but the Q values for the tow samples were quite different (50 and 68.5, respectively). Similar inconsistent observations may be made for samples 9 and 10. Possible cause of this inconsistency could be the partial rupture of the CFRP due to the Hammer impact in most samples. This rupture arbitrarily varied between samples. It may be inferred that Schmidt Hammer is not a reliable tool for hardness measurements on CFRP laminates applied on concrete surfaces.

### 3.2. Pull-Off Testing

The efficacy of the CFRP- Concrete bond can be determined by inspecting the failure modes from the ASTM pull-off testing. Conceptually possible failure modes are shown in Figure 11. The desired mode is type G, indicating that the bond is adequate and the failure is entirely in the concrete substrate. Mode D is a cohesive failure in the epoxy joint, while Mode F is a mixed cohesive failure in concrete and epoxy at the epoxy/concrete interface. These last two modes may be due to inconsistent FRP-concrete adhesion, and could be caused by the presence of surface defects or gravity effect on CFRP. The average pull-off strengths found herein are shown in Table 8.

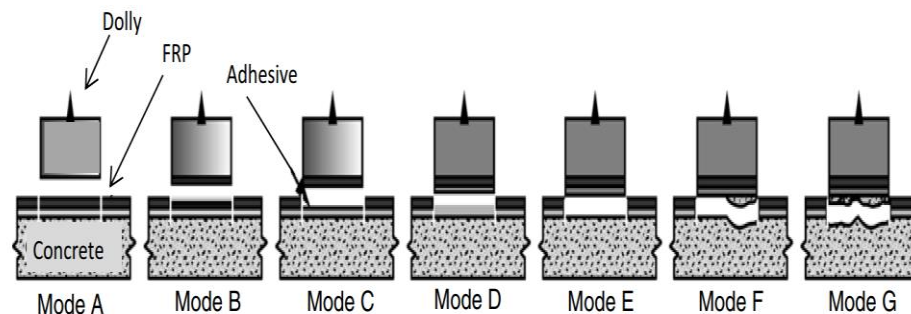
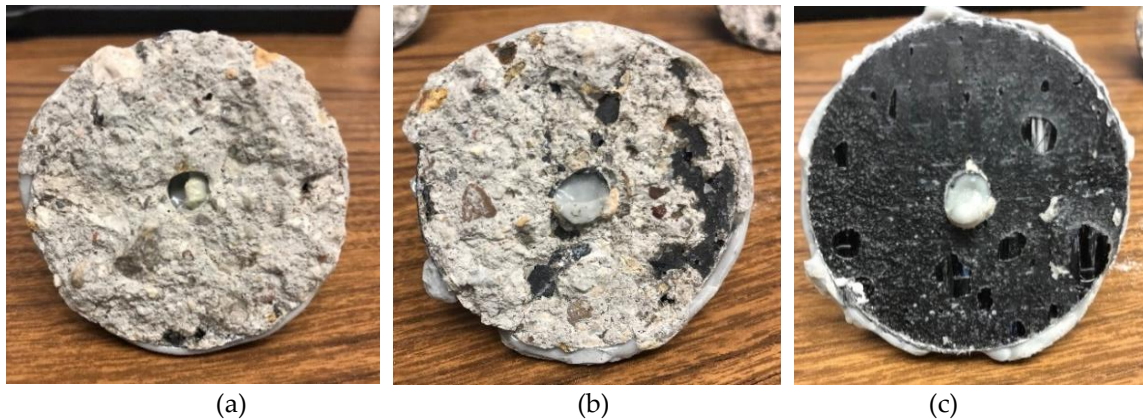


Figure 11. Pull-Off Test Modes of Failure (ASTM D7522/D7522M) (© 2009)

**Table 6.** Pull off Test Results

Sample Number	Average MPa	Failure Mode
1	2.25	Mode F
2	2.17	Mode G
3	1.8	Mode D
4	3.03	Mode G
5	3.05	Mode G
6	2.25	Mode G
7	2.25	Mode F
8	1.77	Mode C
9	2.6	Mode F
10	1.5	Mode F
11	3.01	Mode F

<sup>1</sup>dolly fixture not attached properly, Mode A

**Figure 12.** Pull-off Test Sample Failures. (a) Sample 2, Mode G; (b) Sample 9, Mode F; (c) Sample 8, Mode C

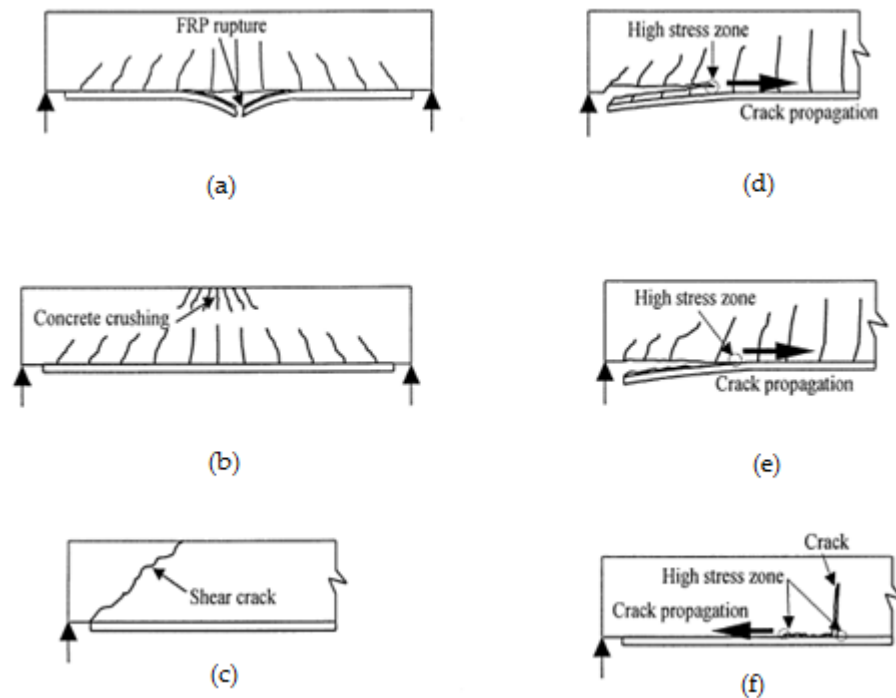


**Figure 13.** Failure modes in CFRP strengthened beams (Teng and Chen, 2007). (a) FRP Rupture; (b) Crushing of Compressive Concrete; (c) Shear Failure; (d) Concrete Cover Separation; (e) Plate End Interfacial Debonding; (f) Intermediate Crack Induced Interfacial Debonding

It is apparent from Table 6 that most pull-off test samples performed relatively well with Mode F – G failures. For samples 3 to 6, the presence of voids did not affect the pull-off results because the dolly was attached to FRP locations that avoided the voided areas. Sample 8 with wet surface had a Mode C failure with lower pull-off strength as expected. Samples with overhead FRP application and unclean surface experienced Mode F failure with partial separation in the concrete substrate (next best to Mode G). Samples 1 – 6 had an average pull-off strength of 2.42 MPa, while the rest of the samples had average strength of 2.22 MPa. Therefore, the pull-off spot check showed the lower tensile strength (by about 9%) of the samples with induced defects (except the ones with voids). It may be noted that the pull-off test is a spot check of FRP bond quality and may not represent an overall indicator of the laminate bonding.

### 3.3. Flexural Testing

Various possible modes of failure for CFRP strengthened concrete beams are shown in Figure 12. If the CFRP laminate ends are properly anchored, failure occurs when the flexural capacity of the beam is reached, by either tensile rupture of the CFRP (Figure 8(a)) or crushing of concrete (Figure 8(b)). For either case, the steel reinforcement generally will not yield at failure.

The failure load and associated failure modes from the flexural testing of samples are presented in Table 2. A typical Mode f failure photographs are shown in Figure 11. The partial FRP debonding with some concrete attached is clearly visible.

**Table 6.** Results from Flexural Test

Sample	Failure Load,KN	Failure Mode (Figure 11)	Maximum Deflection, mm
1	46.2	d	62
2	41.1	f	65
3	55.6	d	94
4	44.9	d	61
5	47.6	d	71
6	44.5	f	46
7	42.7	f	56
8	44.3	f	58
9	52.7	f	79
10	54.7	f	76
11	46.6	f	46

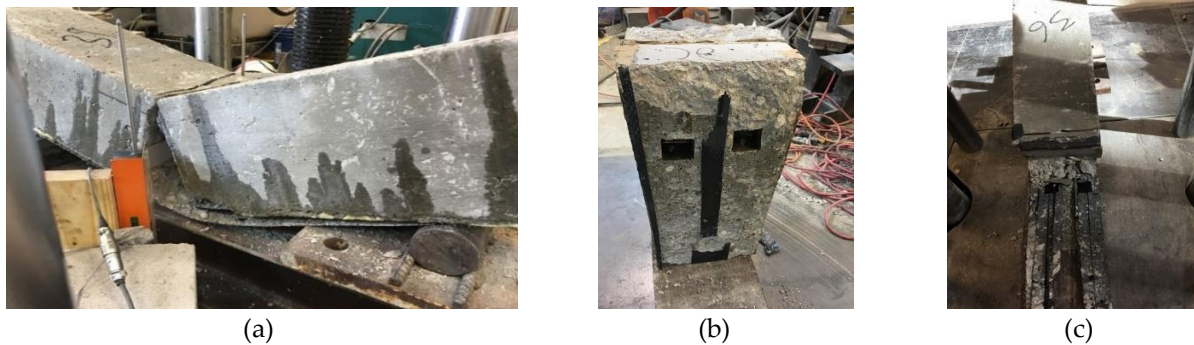


**Figure 14.** Intermediate crack induced interfacial debonding, Sample 7 (a) Failed Sample; (b) Bottom View; (c) Top View

Load vs. maximum deflection plots for all samples are shown in Figures 15 and 16. All graphs show a steep drop in load capacity after the CFRP debonding or cover delamination. It is apparent that all but two samples showed the undesirable plate interfacial debonding failure mode.

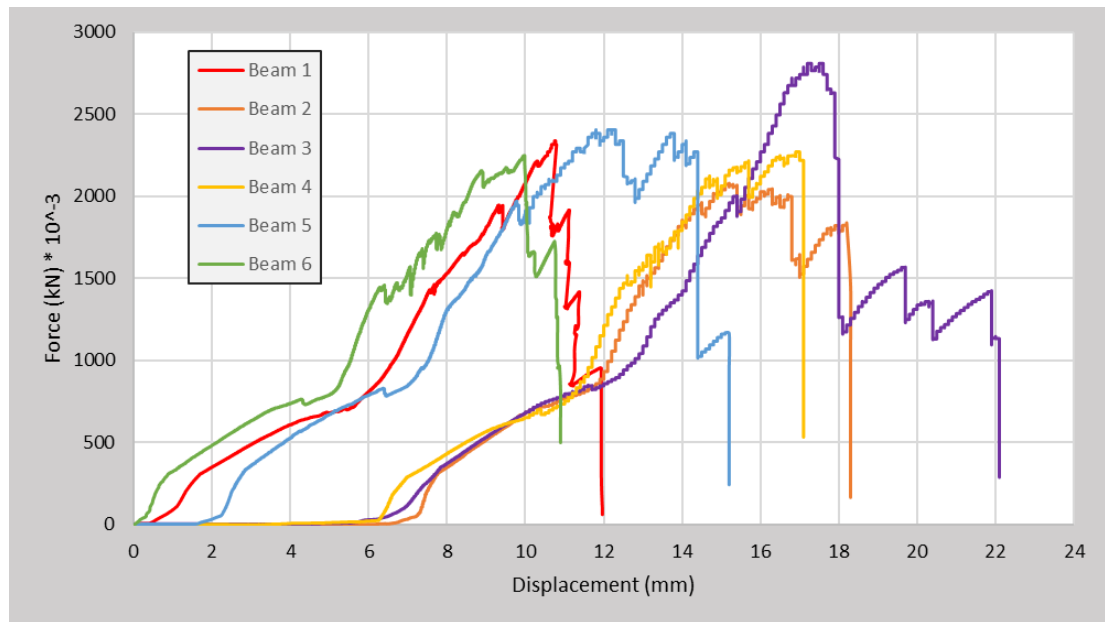


Figure 125. Load vs. Displacement Plots, Samples 1 – 6

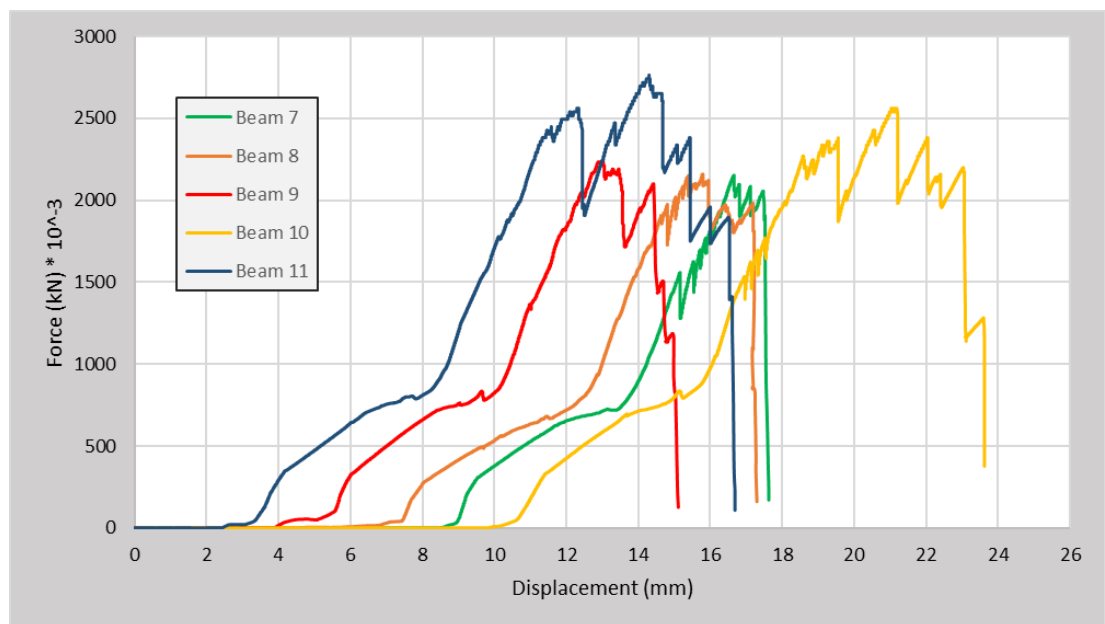


Figure 16. Load vs. Displacement Plots, Samples 7 - 11

The plots show increased displacements at about 13.3 kN, possibly due to the initial engagement of the CFRP laminate in the flexural resistance process. Some samples showed a post-peak reserve strength behavior that included several short rises of load values after the peak performance with increased deflections.

It can be observed that samples 3 - 5 experienced concrete cover separation failure mode, while sample 6 experienced interfacial CFRP debonding. The total void surface areas in the four samples were 400, 1600, 800 and 3200 mm<sup>2</sup>, respectively. Apparently, the larger void size in sample 6 changed the failure mode, causing the lowest failure load and also the lowest maximum vertical deflection in the four samples. The pre-existing and pre-inserted non-bonded areas due to artificial voids herein were 0.23%, 0.89%, 0.45% and

1.78% of the total laminate contact area for the four samples, respectively (based on the contact area of 185,806 mm<sup>2</sup>). The failure load in these four samples were comparable, indicating that there was no appreciable loss of strength due to the presence of surface voids. ACI 440 2R-17 guidelines (ACI 2017) mention that CFRP-concrete delamination of up to 2580 mm<sup>2</sup> or less than 5% of the total laminate area are permissible, and this is corroborated through these observations. However, post-peak load-deflection behavior shows that the peak loads and deflections in the four samples followed trends very similar to the relative surface areas of the voids provided, as shown in Table 7.

Samples 7 and 8, with surface moisture as the induced parameter, had an average failure load of 43.6 kN with average deflections of 57 mm. The load is 3.5% less than the control samples average failure load of 43.7 kN. The ACI 440.2R-17 guidelines and manufacturer guidelines state that the CFRP application must be done in the absence or water. It is apparent that these samples experienced the undesirable plate interfacial debonding failure mode.

Although samples 9 and 10 (with overhead CFRP application) also failed in the interfacial debonding mode, their average failure load of 53.7 kN was significantly more than the control beam average of 43.7 kN. The average maximum deflection for samples 9 and 10 was 77.5 mm, quite a bit greater than the control samples. This was due to the extra epoxy applied in the case of overhead CFRP application. The mixed failure mode F from pull-off tests for these samples confirmed the partial adhesive failures along the concrete interface and sub-quality bonding. The samples also showcased good post-reserve strength and deformation after the delamination of CFRP laminate (Figure 16). Although the bond quality was not good, the effect of a combination of epoxies increased the beam strength.

Sample 11 (with unclean surface condition) had a failure load that was 6.7% less than the control samples. The sample also had a relatively lower maximum failure deflection. The failure modes from the pull-off test and bending test indicated an inadequate quality CFRP bond. The post-peak residual strength and deflections were also substantially less than the control samples.

ACI 400.2R-17 (ACI 2017) does not suggest any strategies for the NDE of the bond quality between FRP laminate and concrete substrate, nor does it discuss the effects of surface defects. Therefore, this study may serve as a valuable reference for inspection and evaluation of such interfaces for quality control.

#### 4. Conclusions

The following conclusions may be made based on the results from this study:

1. Non-destructive evaluation (NDE) can be used as an effective tool to evaluate the quality of bond between CFRP-concrete, thus assisting in the identification of poor workmanship and/or environmental effects that may affect the bond.
2. The effect of concrete surface voids, surface wetness, upward application of CFRP and surface cleanliness on the quality of the CFRP-concrete interfacial bond can be conclusively detected through the infrared thermography process. Quantification of any reduction in the failure capacity of such concrete flexural members is also possible.
3. It was found that the Schmidt Hammer approach may not be a reliable tool for hardness measurements on CFRP surfaces bonded to concrete substrates. This could be due to the partial rupture of the CFRP laminates under the impact of the Hammer, causing inconsistent results.
4. The ASTM Pull-Off Testing can be an effective tool to spot check the integrity and in-situ tensile strength of the applied CFRP laminate. Most pull-off test samples performed relatively well in this study, with complete or partial failures in the concrete substrate. Wet surface, unclean surface and upward CFRP application caused 9% average lowered pull-off strength, as compared to samples

without such defects, as expected. It may be noted that the pull-off test is a spot check of FRP bond quality and may not represent an overall indicator of the laminate bonding quality.

5. Wet surface, unclean surface and upward CFRP application may result in inadequate CFRP-concrete bond quality that can result in premature bond failure at the interface, as opposed to concrete cover separation failure.
6. Increased surface area (at about 1.78% of the laminate contact area) of any air voids below the applied CFRP laminate may decrease the bond capacity and also cause the undesirable interfacial CFRP debonding failure mode, as opposed to concrete cover separation failure mode. However, this decrease is acceptable, because according to ACI 440 2R-17 guidelines, FRP delamination below 5% of the total laminate area may be neglected in design, as this may not impact the bond capacity significantly. Peak loads and deflections in the samples with voids were proportional to the relative surface areas of the voids provided.
7. Concrete surface moisture may hinder proper CFRP-concrete bonding and lower the bond capacity, however, the decrease is not very high, in the range of 3.5%. It is apparent that these samples experienced the undesirable plate interfacial debonding failure mode. Relevant specifications and manufacturer guidelines suggest that the concrete surface should be dry for proper CFRP application.
8. Overhead CFRP application, the most common type used for concrete rehabilitation, may result in the CFRP interfacial debonding failure mode. This study showed the difficulty of overhead placement due to the reverse gravity effect with manufacturer's recommended epoxy thickness applications. An extra epoxy layer was necessary for proper CFRP adhesion. This can significantly increase the bond capacity and maximum beam deflections.
9. Dust and laitance on the concrete surface can adversely affect the interfacial CFRP bond quality, to the tune of a bond strength reduction up to 6.7%. Failure modes associated with this surface defect may also show inadequate quality of the CFRP bond. Post-peak residual strength and deformations are also lower in these cases.

**Acknowledgments:** The study herein was performed under a contract from the Texas Department of Transportation. Support from the Civil Engineering Department at the University of Texas at Arlington for laboratory facilities and equipment is gratefully acknowledged.

## References

- [1] Ekenel, M.; Myers, J. Nondestructive Evaluation of RC Structures Strengthened with CFRP Laminates Containing Near-Surface Defects in the form of Delaminations. *Science and Engineering of Composite Materials* 2011 14(4), pp. 299-316. Retrieved 31
- [2] Frédéric Taillade; Marc Quiertant; Karim Benzarti; Jean Dumoulin; Christophe Aubagnac. Non-destructive Evaluation of CFRP Strengthening Systems Bonded on RC Structures Using Pulsed Stimulated Infrared Thermography, 2012. 10.5772/27488.
- [3] Valluzzi, M. R.; Grinzato, E.; Pellegrino, C.; Modena, C. IR thermography for interface analysis of CFRP laminates externally bonded to RC beams. *Mater. Struct.* 2009 42(1), 25–34.
- [4] Jackson D; Islam M; Alampalli S. (2000). Feasibility of evaluating the performance of fiber reinforced plastic (CFRP) wrapped reinforced concrete columns using ground penetrating RADAR (GPR) and

- infrared (IR) thermography techniques. Structural Materials Technology IV-An NDT Conference, 390-395.
- [5] Halabe UB; Vasudevan A; Klinkhachorn P; GangaRao HV. Detection of subsurface defects in fiber reinforced polymer composite bridge decks using digital infrared thermography. *Nondestructive Testing and Evaluation* 2007 22(2-3), 155-175.
- [6] Shih JKC; Tann DB; Hu CW; Delpak R; Andreou E. Remote sensing of air blisters in concrete-CFRP bond layer using IR thermography. *International Journal of Materials and Product Technology* 2003 19(1-2), 174-187.
- [7] D. H. Chen; A. Wimsatt. Inspection and condition assessment using ground penetrating radar. *Journal of Geotechnical and Geoenvironmental Engineering* 2010 vol. 136, no. 1, pp. 207–213.
- [8] Tzu-Yang Yu; Oral Büyüköztürk. A far-field airborne radar NDT technique for detecting debonding in GCFRP-retrofitted concrete structures. *NDT & E International* Volume 41, Issue 1, 2008, Pages 10-24.
- [9] S. Park; S. -K. park. Debonding condition monitoring of a CFRP laminated concrete beam using piezoelectric impedance sensor nodes, *Fracture Mechanics of Concrete and Concrete Structures - Assessment, Durability, Monitoring and Retrofitting of Concrete Structures*, Korea Concrete Institute, Seoul, 2010, ISBN 978-89-5708-181-5.
- [10] J. Brown; H.R. Hamilton III. NDE of reinforced concrete strengthened with fiber-reinforced polymer composites using infrared thermography, *InfraMation*, ITC 092 A 2003-08-15, ITC 092 A 2003-08-15.
- [11] American Society for Standard Testing and Materials (ASTM) (2015). *Standard Specification for Epoxy-Resin-Base Bonding Systems for Concrete*, ASTM C881/C881M-15, West Conshohocken, PA.
- [12] American Association of State Highway Transportation Officials (AASHTO) (2013). *Specification for Epoxy Resin Adhesives*. AASHTO M 235M/M235, Washington, D.C.
- [13] ACI (American Concrete Institute). (2017). "Guide for the design and construction of externally bonded CFRP systems for strengthening concrete structures." ACI 440.2R, Farmington Hills, MI.
- [14] ICRI Committee 310, "Selecting and Specifying Concrete Surface Preparation for Sealers, Coatings, and Polymer Overlays (ICRI Guideline No. 310.2-97)," International Concrete Repair Institute, Rosemont, IL, 2002, 41 pp.
- [15] ASTM, Standard Test Method for Pullout Strength of Hardened Concrete, ASTM C900-15, 2015. West Conshohocken, PA



© 2018 by the authors; American Journal of Life Science Researches, USA. This is an open access article distributed under the terms and conditions of the Creative Commons Attribution (CC-BY) license (<http://creativecommons.org/licenses/by/4.0/>).